Key Engineering Materials
ISSN: 1662-9795, Vol. 926, pp 2012-2021
doi:10.4028/p-73lq3w

Submitted: 2021-12-08
Revised: 2022-01-27
Accepted: 2022-01-28
Online: 2022-07-22

Work Hardening of Metallic Sheets under Tension-Compression and Simple Shear Reverse Loading

D.J. Cruz[1,a*], A.F.G. Pereira[3, b], V.M. Simões[3,c], R.L. Amaral[1,d], A.D. Santos[2,e] and M.C. Oliveira[3,f]

[1]INEGI, Inst. Science and Innovation in Mechanical and Industrial Engineering, Porto, Portugal

[2]FEUP, Faculty of Engineering, University of Porto, Porto, Portugal

[3]CEMMPRE, Dep. Mechanical. Engineering, University of Coimbra, Coimbra, Portugal

[a*]dcruz@inegi.up.pt, [b]andre.pereira@uc.pt, [c]vasco.simoes@uc.ptl
[d]ramaral@inegi.up.pt, [e]abel@fe.up.pt, [f]marta.oliveira@dem.uc.pt

Keywords: Miniaturized tension-compression tests, Reverse shear tests, Kinematic hardening

Abstract. The hardening models have a significant influence on the accuracy of finite element analysis (FEA). Although, isotropic hardening models are the most widely used, it is known that kinematic hardening models (describing the Bauschinger effect and permanent softening) can significantly improve the accuracy of FEA results. However, when considering sheet metal materials, the parameters of kinematic hardening models are difficult to identify due to the challenges of obtaining experimental results from test with strain path inversions. This work considers an experimental procedure that enables the analysis of the mechanical behaviour of sheet metal materials submitted to reverse loadings. A miniaturized test device was developed to perform tension and compression tests, with reverse loadings, for sheet metal materials. This specimen design has two main advantages: (1) reduces buckling during compression (compared to standard tensile test specimens) and, consequently, (2) enables the characterization of the mechanical behaviour under reverse tension-compression strain paths changes. The small size of the specimens, with 2 x 2 mm gauge area, poses the main challenge of the current methodology, namely the measurement of the strain field distribution using the Digital Image Correlation (DIC) technique. The results obtained from tension-compression tests with mini-specimens are validated by comparison with standard tensile and shear (reverse loading) tests.

Introduction

The challenge given to the automotive industry regarding energy efficiency and low consumption vehicles has resulted in the demand for increasingly lighter construction components [1, 2]. The use of new materials for weight reduction is essential to address these issues. Instead of conventional steels, advanced high-strength steels (AHSS) and aluminium alloys have been used to meet the above goal. However, springback is more pronounced in these materials than in conventional steels due to their unique material properties, which lead to additional processing difficulties and costs for industrial application [3]. It is well known that in order to accurately predict springback, a material model must precisely describe the hardening behaviour that occurs during load reversal solicitations, including the Bauschinger effect, transient behaviour, permanent softening, and work hardening stagnation, as schematically shown in Figure 1.

Nonlinear isotropic/kinematic hardening models are an effective way to predict springback. However, the accuracy of these material models is highly dependent on the experimental test methodology and parameter calibration procedure adopted. Experimentally the parameter calibration is done based on tests with load path changes or cyclic tests. Several experimental methodologies have been used to characterize load path changes in sheet metal materials. These experiments can be classified into three main categories: (i) bending-unbending test; (ii) in-plane cyclic shear test; and (iii) in-plane uniaxial tension-compression test. There is no consensus about which is the best method, since each has its one advantages and disadvantages.

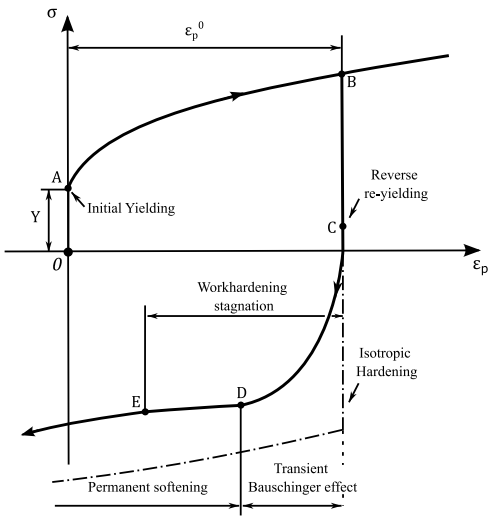

Figure 1. Schematic illustration of stress-strain response during forward and reverse deformation.

In bending-unbending test, the inner/outer layers experience compression-tension/tension–compression loadings [4]. Therefore, this test can be used to evaluate the hardening behaviour under strain path inversions. This test was introduced by Yoshida et al. [5], using a uniform bending device for cyclic bending. Later Geng et al. [6] developed a three-point cyclic bending that was later improved by Omersphahic et al. [7]. Compared with the in-plane cyclic shear test and the in-plane tension-compression test, cyclic bending is less common. This can be related with some disadvantages: firstly, it is hard to identify the Bauschinger effect at large strains; secondly, the stress and the strain are gradient-distributed at the measured area; lastly, the hardening properties of the material under one-dimensional loading cannot be directly determined from the load-displacement curve and an inverse method is required. The main advantage is that the deformation mode in this test is similar to some forming processes, where the sheet metal is formed over several radii in the die [8].

The in-plane cyclic shear test is commonly used by several authors to characterize the kinematic hardening of sheet metals [9-11]. This test allows the evaluation of large strain responses under reverse loadings. Compared with the tension-compression test, the cyclic shear test can avoid tensile necking and buckling, however presents some disadvantages. firstly, the strain in the sheared gauge region can be non-homogeneous and very often, it is difficult to measure; secondly, the stress state in simple shear test is complicated and it results in the fact that the planar anisotropy influences the measured shear stress of cyclic simple shear test [12].

The uniaxial in-plane tension-compression test caught attention during the last decade. The advantage of the uniaxial test is that the strain distribution is uniform, and therefore, it is easy to find the material response. Unfortunately, a uniaxial compressive stress state may cause buckling in sheet metal materials, for small compressive strains. In order to avoid buckling during the compression phase, different solutions have been developed over the years, which can be divided into three groups: (i) pack method, using a set of specimens packed together in the thickness direction; (ii) single sheet with a lateral support system; and (iii) miniaturized test samples with low gauge-length/thickness ratio.

The pack method consists of packing together a set of specimens (in thickness) as a unique specimen. This strategy reduces the length/thickness ratio, reducing the probability of buckling under compression. Aitchison et al. [13] and Jackman [14], joined flat sheet metal tensile specimens in a unique pack and submitted them to compression. In addition to flat tensile test specimens with bone-shaped contours, rectangular sheet metal strips have been also used as specimen geometries [15]. Yoshida et al. [16] used a variation of the pack method, where five specimens were glued together, and then covered with clamping plates. However, the pack method requires a large number of specimens and a complex preparation. Therefore, some authors prefer using a single sheet with a lateral support system. Boger et al. [17, 18] used two solid support plates to “sandwich” the specimen with a constant restraining side force, generated by a hydraulic cylinder. An exaggerated dog-bone specimen was optimized to suppress buckling in the thickness direction (T-buckling), in the

unsupported gap (L-buckling), and in the width direction (W-buckling). Sekine and Kuwabara [19] have introduced a device with two sets of fork-shaped supports to eliminate the uncovered area in tensile-compressive relative movements. This design allowed the entire length of the specimen to be supported, because, as the sample is compressed, the male and female dies slide past each other.

Buckling in compression is mainly influenced by its gauge-length/thickness ratio. Therefore, test methods with miniaturized specimens were recently proposed as a powerful solution to study the compression behaviour of the material. Tritschler et al. [20] tested a 1.2 mm thickness titanium alloy in compression using specimens of 2.5 mm length by 2 mm width, attaining about 2% of compressive strains. Hußnätter [21] used a specimen geometry with a 2 mm length by 2 mm width for the characterization of the magnesium alloy AZ31, achieving about 5% of compressive strains before the specimen buckles. Cruz et al. [22] have analysed the mechanical behaviour of sheet materials, comparing miniaturized test samples with macro standard tensile specimens, concluding that miniaturized test samples can accurately describe the mechanical material behaviour and thus, they can be used to evaluate the mechanical behaviour of sheet metal materials during reverse loadings.

The present work focuses on the experimental characterization of the mechanical behaviour of sheet metal materials during reverse loadings, aiming to describe phenomena such as the Bauschinger effect and permanent softening. The results obtained from tension-compression tests with mini-specimens are validated by comparison with shear tests (reverse loading) and tensile tests with standard specimens. The future goal is to improve the identification of material parameters of kinematic hardening models and, consequently, improve the accuracy of results on FEA of sheet metal materials. Section 2 presents the tested alloys and the experimental devices used. Section 3 presents the experimental results, which are compared and discussed in section 4. Finally, the conclusions are presented in section 5.

Materials and Methods

In the present work two different sheet metal materials were tested: DP600 and AA5754-H11, with a thickness of 0.8 mm and 1 mm, respectively. DP600 is a dual-phase steel with a good combination of strength and ductility due to its martensite islands in a ferrite matrix. On the other hand, AA5754-H11 is a series 5000 aluminium alloy subjected to H11- temper, i.e. annealing followed by air cooling. The chemical composition of both materials is listed in Table 1. The elastic behaviour was described assuming literature reference values: Poisson's ratio of 0.3 for both materials; and Young's modulus of 210 GPa and 70 GPa for the DP600 and AA5754, respectively.

Table 1. Chemical composition of the DP600 dual-phase steel and AA5754 H11 aluminium alloy.

Element [%]	C	Si	Mn	P	S	Cr	Ni	V	Cu	Al	Nb	B	N	EC[1]
DP600	0.089	0.20	0.85	0.014	0.004	0.03	0.03	0.01	0.01	0.046	0.019	0.0003	0.004	0.24
Element [%]	**Si**		**Fe**		**Cu**		**Mn**		**Mg**		**Cr**	**Zn**	**Ti**	**Al**
AA5754-H11	0.4		0.4		0.1		0.5		2.6-3.6		0.3	0.2	<0.15	balance

[1] $EC = C + \frac{Mn}{6} + \frac{Ni+Cu}{15} + \frac{Cr+Mo+V}{5}$

Experimental mini tension-compression tests and shear tests were performed for both alloys, using two different devices described later. The grip was controlled with a constant displacement in order to achieve a strain rate of about 10^{-3} s^{-1} in all the tests. Both alloys were tested at room temperature (≈20 ºC), considering specimens cut in alignment with the sheet rolling direction. Finally, several tests were performed for each material to guarantee the repeatability of the results. However, for a clear analysis of the stress-strain curves, only one result for each type of specimen is presented.

The experimental tension-compression tests were performed using an equipment specifically designed for miniaturized specimens - Mini Sample Tester Device (MSTD), see Figure 2 (a) [22, 23]. The geometry of the miniaturized specimen was optimized to reduce the buckling effect in the thickness direction, see Figure 2 (b). The MSTD layout allows all components to be on a common plane, which is advantageous for a precise alignment of the specimen during the test. Consequently, the appearance of undesirable bending moments is minimized, especially in compression, which is

also essential to prevent the buckling of the specimen. The force was measured using an "S"- type load cell, while the strain fields were acquired by digital image correlation (DIC) technique. The DIC images were taken at a frequency of 20 Hz with a 5 MPixel camera (BasleracA2440-75um, 2448x2048 pixels) in combination with a telecentric lens (InfaimonOPE-TC-23-09,45mm). Finally, MSTD results were compared with macro tensile specimens tested on an Instron 5900R (300 kN) according to ISO 6892-1:2016 [24].

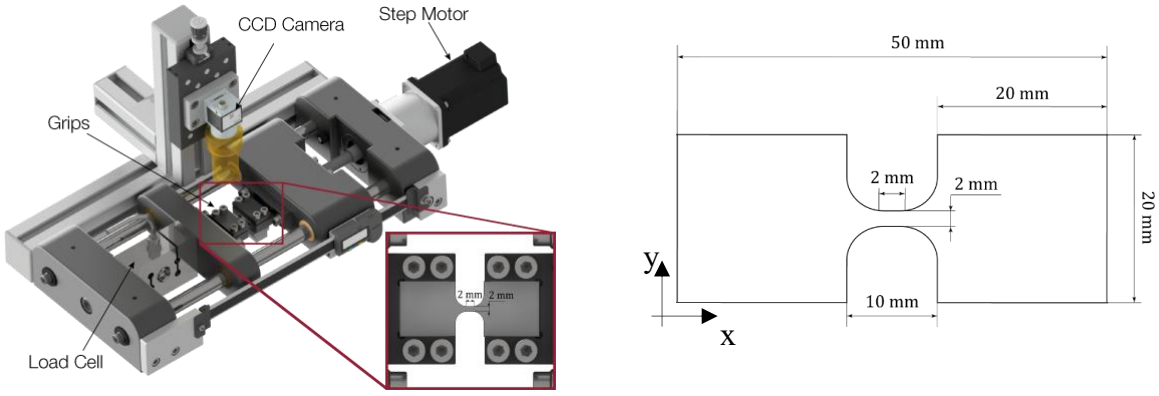

(a) (b)

Figure 2. Micro tension-compression device: (a) MSTD setup, and; (b) geometry of the miniaturized specimen.

The experimental shear tests were performed in a universal tensile test machine Shimadzu 100kN, using a shear device based on the design of Yoon et al. [25] (see Figure 3 (a)). The geometry of shear specimens has a length of 34.6 mm and a width of 13 mm, as shown in Figure 3 (b). In this apparatus, the shear specimen is fixed by two grips that are subjected to a parallel displacement, leading to shear deformation in a gauge area of 3 mm wide. The shear stress, τ_{xy}, was calculated by the equation:

$$\tau_{xy} = \frac{F}{L_0 \times t_0}, \tag{1}$$

where: F is the load resulting from the grip displacement, L_0 is the initial specimen length, and t_0 is the initial specimen thickness. During the test, the shear strain was measured using the DIC technique, at a frequency of 1 Hz, using system Aramis 5M from GOM with cameras resolution of 2448x2050 pixels.

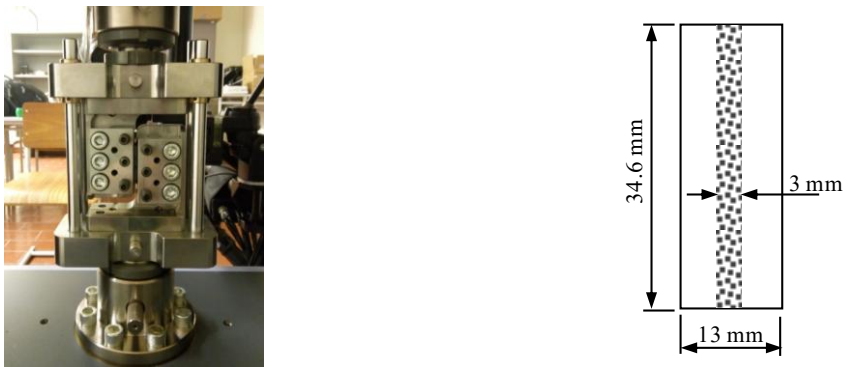

(a) (b)

Figure 3. Shear device: (a) setup on a universal tensile test machine; (b) geometry of shear specimen.

Experimental Results

The true stress-strain curves of the monotonic uniaxial tensile test comparing mini and macro specimens are presented in Figure 4, for: (a) DP600 and (b) AA5754. Globally, the results of the miniaturized specimen are in very good agreement with the macro tensile test. In fact, for both materials, the elastic part and the hardening behaviour is very similar for both specimens geometries, which is in agreement with previous findings [22].

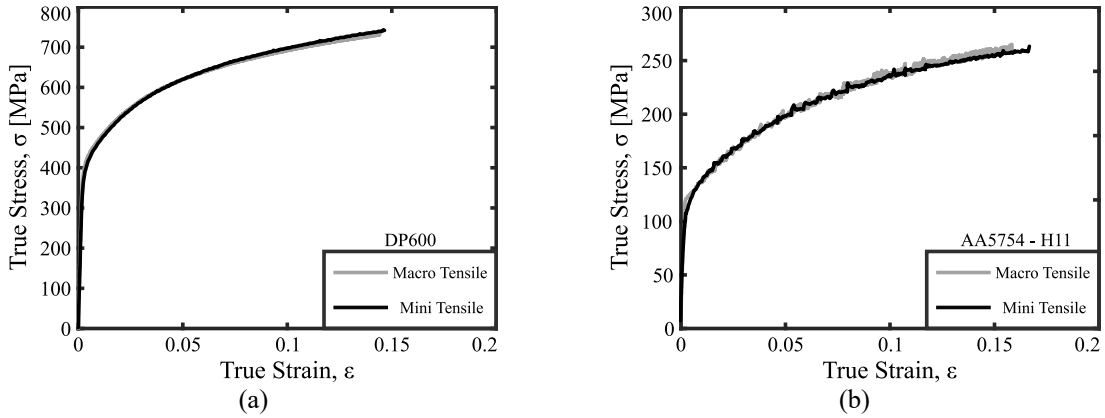

(a) (b)

Figure 4. Monotonic uniaxial tensile test comparing mini and macro specimens: (a) DP600 and (b) AA5754.

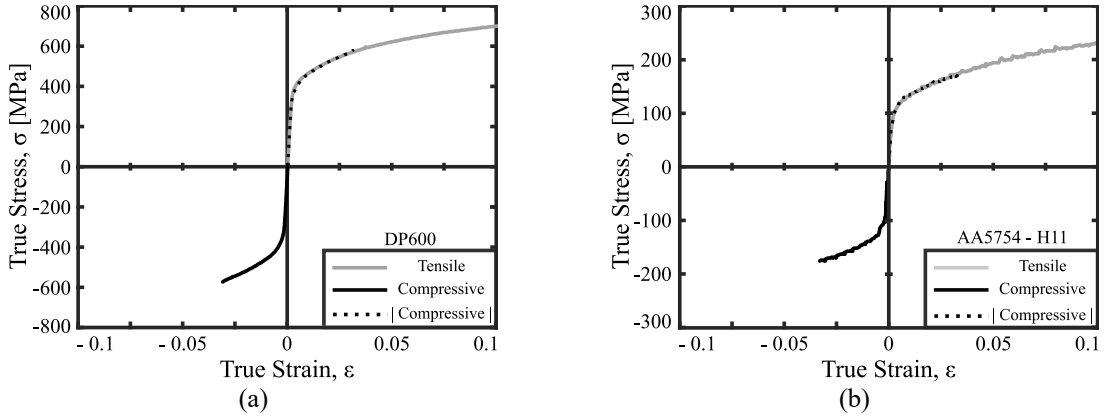

(a) (b)

Figure 5. Micro monotonic uniaxial test of tensile and compression specimens: (a) DP600 and (b) AA5754.

Figure 5 shows the comparison between tension and compression using the miniaturized specimens, for: (a) DP600 and (b) AA5754. Additionally, the absolute compressive true stress-strain values are also presented (dotted line) to simplify the comparison between compression and tension behaviours. The results show that both materials have a similar hardening evolution in tension and compression since the absolute compressive curve (dotted line) closely followed the curve obtained in the mini tensile test. In compression the maximum strain values, of about 0.03-0.04, are lower than in tension due to the buckling phenomenon. This is corroborated by Figure 6 which shows the strain distribution in the specimen at the tensile strength values, for the: monotonic tensile test, and, monotonic compression test.

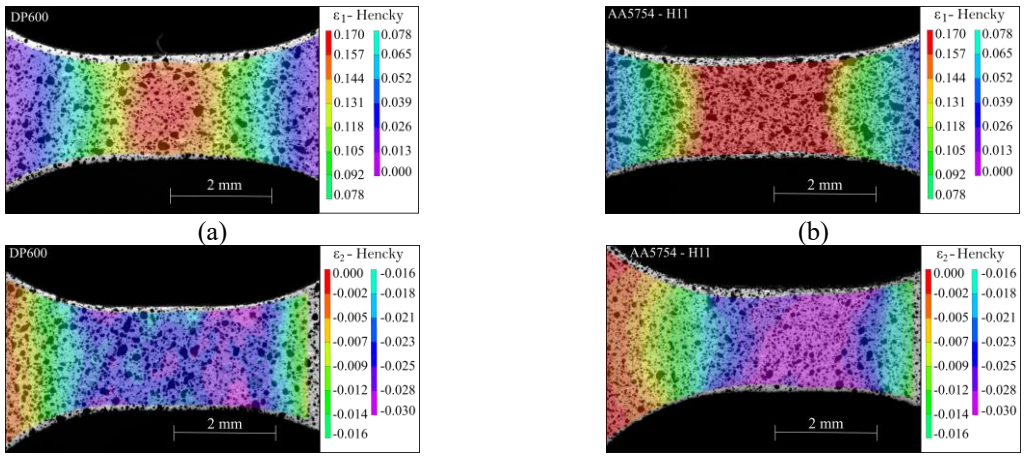

(a) (b)

(c) (d)

Figure 6. Strain distribution in the specimen: (a) DP600 monotonic tensile test; (b) AA5754 monotonic tensile test; (c) DP600 monotonic compression test; (d) AA5754 monotonic compression test.

The reverse stress-strain curves for tension-compression and shear tests are presented in Figure 7 and Figure 8, respectively. In both figures, the monotonous stress-strain curves are presented for comparison. In tension-compression and shear tests, the reverse curve matches the monotonous one, which confirms the repeatability of the experimental results. The tension-compression test was performed submitting both alloys to a tensile stress followed by a compression stage until the buckling phenomenon becomes evident. The reverse loading occurs for an equivalent plastic strain value of about 5% ($\varepsilon \approx 0.05$). The reverse shear tests were performed imposing the load inversion for a shear strain value of about 10%, which corresponds to an equivalent plastic strain value of about 5%. Thus, the equivalent strain is similar before and after reverse load for both tests. Finally, since experimental test devices need to be controlled in Force (load) values, the precision of the equivalent plastic strain at the load inversion is small. The comparative analysis between the tension-compression and reverse shear tests will be discussed in the next section.

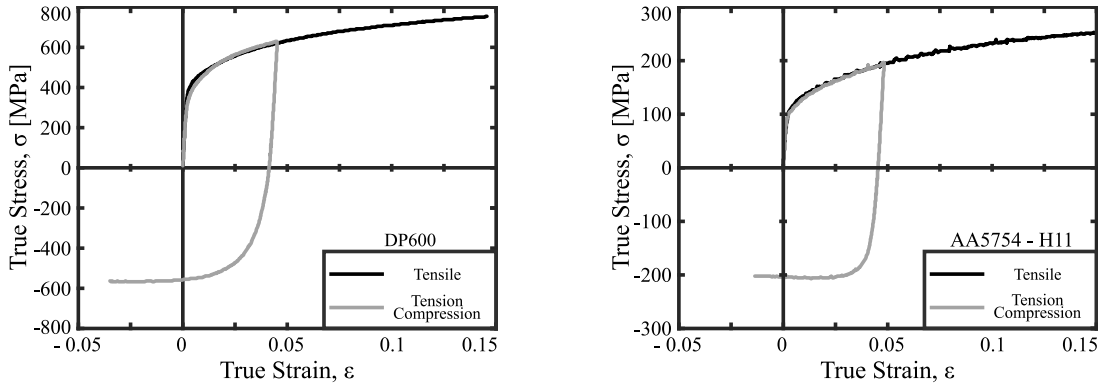

Figure 7. Reverse-loading stress-strain curves of tension-compression test: (a) DP600 and (b) AA5754.

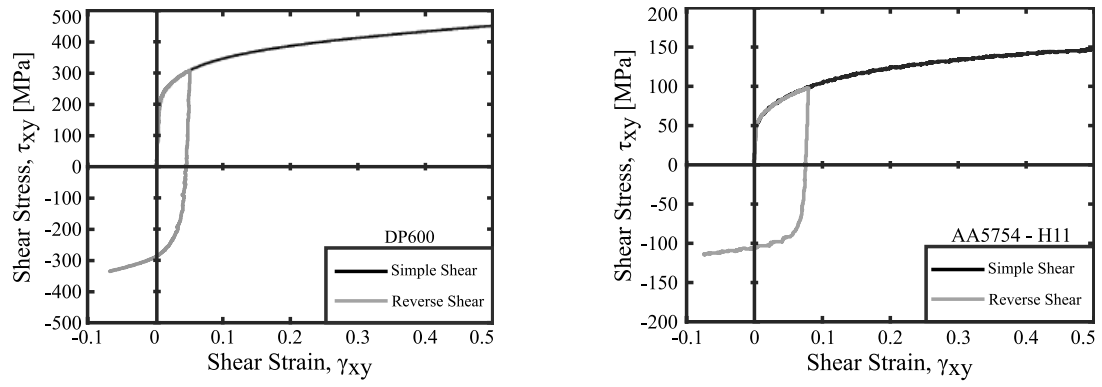

Figure 8. Reverse-loading stress-strain curves of the shear test: (a) DP600 and (b) AA5754.

Discussion and Comparison with Numerical Results

To directly compare the shear test with the uniaxial tension-compression test, the shear stress, τ_{xy}, and the shear strain, γ_{xy}, needs to be converted to equivalent stress, σ_e, and equivalent strain, ε_e. Usually, the von Mises yield criterion is the most used for its simplicity. However, this yield criterion is unable to accurately model the shear and tensile results, due to the anisotropy of the metal sheets, as reported by Kang et al. [26]. Therefore, the plastic behaviour was also modelled using the yield criterion proposed by Cazacu et al. [27], hereafter designated by CPB06. This criterion is more flexible than the von Mises criterion and, can describe the orthotropic behaviour and the tension-compression asymmetry. The CPB06 yield criterion is defined as follows:

$$Y = B[(|s_1| - ks_1)^a + (|s_2| - ks_2)^a + (|s_3| - ks_3)^a]^{1/a}, \quad (2)$$

where Y is the flow stress, which is equal to the equivalent stress under load condition; k and a are material parameters; and s_i (i = 1 to 3) are the principal values of $\mathbf{s} = \mathbf{C} : \boldsymbol{\sigma}'$. The fourth-order tensor $\mathbf{C}$, operating on the deviatoric Cauchy stress tensor $\boldsymbol{\sigma}'$, is given by:

$$\mathbf{C} = \begin{bmatrix} C_{11} & C_{12} & C_{13} & 0 & 0 & 0 \\ C_{12} & C_{22} & C_{23} & 0 & 0 & 0 \\ C_{13} & C_{23} & C_{33} & 0 & 0 & 0 \\ 0 & 0 & 0 & C_{44} & 0 & 0 \\ 0 & 0 & 0 & 0 & C_{55} & 0 \\ 0 & 0 & 0 & 0 & 0 & C_{66} \end{bmatrix}, \tag{3}$$

where, C_{ij} (i,j = 1 to 6) are material parameters. B is a constant, that makes the equivalent stress (defined in Eq. (2)) equal to the flow stress in uniaxial tension along the rolling direction (RD), when it is defined as follows:

$$B = \left[\frac{1}{[(|\phi_1| - k\phi_1)^a + (|\phi_2| - k\phi_2)^a + (|\phi_3| - k\phi_3)^a]}\right]^{1/a}, \tag{4}$$

with, $\phi_i = (2/3)C_{i1} - (1/3)C_{i2} - (1/3)C_{i3}$ (i = 1 to 3). The CPB06 constitutive parameters were identified based on the following experimental data: R-values and yield stresses from tensile tests cut at 0º, 22.5º, 45º, 67.5º and 90º with the RD; yield stresses from shear tests cut at 0º and 45º with the RD; and the biaxial yield stress obtained from the bulge test. The identified parameters for the DP600 and AA5754 are shown in Table 2.

Table 2. Constitutive parameters identified for the materials DP600 and AA5754.

	C_{11}	C_{22}	C_{33}	C_{44}	C_{55}	C_{66}	C_{12}	C_{13}	C_{23}	a	k
DP600	1	0.896	4.608	1	1	3.044	-2.095	0.115	0.184	8	0
AA5754	1	1.165	1.072	1	1	1.076	0.088	-0.041	0.021	4	0

Figure 9 shows the stress strain curves of the monotonous tensile test compared to the equivalent shear tests results calculated using the von Mises and the CPB06 yield criteria. The equivalent stress-strain curves obtained with the CPB06 yield criterion are more accurate than those obtained with the von Mises one. This is a clear indication that the material's behaviour is better described by the CPB06 yield criterion. However, for the AA5754-H11, even the more flexible CPB06 yield criterion still is not able to fully describe the material behaviour.

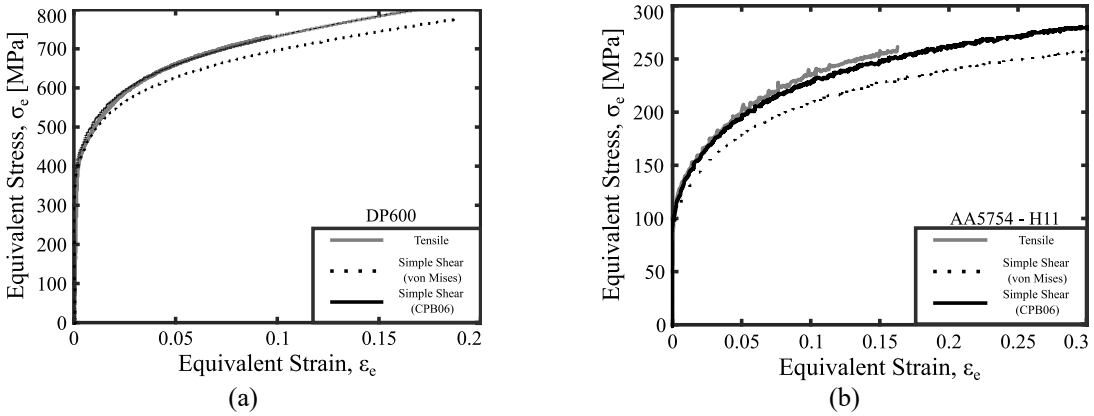

(a) (b)

Figure 9. Equivalent strss-strain curves for tensile tests and shear tests: (a) DP600 and (b) AA5754.

The equivalent reverse shear results obtained with the CPB06 yield criterion are presented in Figure 10 for: (a) DP600 and (b) AA5754-H11. As comparison, each figure also presents the equivalent simple shear curve and the tension-compression curve (considering reverse loading at

$\varepsilon \approx 0.05$). Both tests enable to capture a similar transient Bauschinger effect (see Figure 1) for both alloys. However, for higher strain values after inversion, it is visible a different hardening behaviour, i.e., a different permanent softening and work hardening stagnation. At this moment it is important to highlight that for a better comparison between the tests, it would be important to guarantee a more similar value of equivalent plastic strain at the inversion. However, experimentally this agreement is difficult to achieve because it is dependent on many external factors, e.g. the machine control and a possible slip of the specimen during the test.

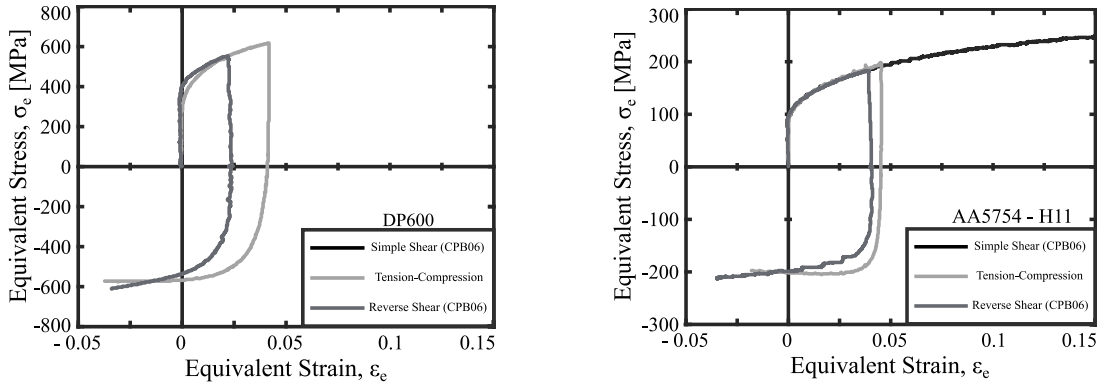

(a) *(b)*

Figure 10. Equivalent reverse-loading stress-strain curves for CPB06 criterion: (a) DP600 and (b) AA5754.

Conclusions

Aiming to improve the accuracy of FEA results on sheet metal forming, this work uses a Mini Sample Tester Device for tension and compression tests (with reverse loading) as a solution for the identification of kinematic hardening models. The use of mini-specimens minimizes buckling during compression (compared to standard tensile test specimens) and, consequently, allows to characterize the mechanical behaviour under reverse tension-compression strain paths changes. Two materials were selected, namely DP600 and AA5754-H11 with a thickness of 0.8 mm and 1 mm, respectively. Several experimental tests were carried out in the selected materials: monotonic uniaxial tensile and compressive tests; uniaxial tests with reverse loading (tensile followed by compressive); simple shear and shear test with reverse loading.

The monotonic tensile test using miniaturized specimens presented a good agreement with the standard tensile test (macro specimens) which confirms the use of mini specimens to evaluate the hardening behaviour of the materials. Additionally, it is seen that compression stress-strain curves are similar to the tensile ones, meaning that the device can be used to evaluate the tension-compression asymmetry. Nevertheless, the hardening behaviour can only be characterized for compressive strains up to 0.02-0.04. Regarding the comparison between tension-compression tests and reverse shear tests, the use of the CPB06 yield criterion proves to be more accurate to convert the shear results in equivalent ones, when compared with an isotropic criterion. The comparison using equivalent stress-strain curves shows that the results are promising, since a similar transient Bauschinger effect is observed on both tests.

Acknowledgements

The authors gratefully acknowledge the financial support of the projects POCI-01-0145-FEDER-030592 (PTDC/EME-EME/30592/2017), POCI-01-0145-FEDER-031243 (PTDC/EME-EME /31243/2017), POCI-01-0145-FEDER-031216 (PTDC/EME-EME/31216/2017) and UIDB/00285 /2020 financed by the Operational Program for Competitiveness and Internationalization, in its FEDER/FNR component, and the Portuguese Foundation of Science and Technology (FCT), in its State Budget component (OE).

References

[1] Berladir, K., et al., *Modern materials for automotive industry.* Journal of engineering sciences, 2017. **4**: p. F8-F18.

[2] Ghosh, M., A. Ghosh, and A. Roy, *Renewable and Sustainable Materials in Automotive Industry*. 2019. p. 1-18.

[3] Hilditch, T.B., T. de Souza, and P.D. Hodgson, *2 - Properties and automotive applications of advanced high-strength steels (AHSS)*, in *Welding and Joining of Advanced High Strength Steels (AHSS)*, M. Shome and M. Tumuluru, Editors. 2015, Woodhead Publishing. p. 9-28.

[4] Eggertsen, P.-A. and K. Mattiasson, *On the modelling of the bending–unbending behaviour for accurate springback predictions.* International Journal of Mechanical Sciences - INT J MECH SCI, 2009. **51**: p. 547-563.

[5] Yoshida, F., M. Urabe, and V.V. Toropov, *Identification of material parameters in constitutive model for sheet metals from cyclic bending tests.* International Journal of Mechanical Sciences, 1998. **40**(2): p. 237-249.

[6] Geng, L., Y. Shen, and R.H. Wagoner, *Anisotropic hardening equations derived from reverse-bend testing.* International Journal of Plasticity, 2002. **18**: p. 743-767.

[7] Omerspahic, E., K. Mattiasson, and B. Enquist, *Identification of material hardening parameters by three-point bending of metal sheets.* International Journal of Mechanical Sciences, 2006. **48**(12): p. 1525-1532.

[8] Ghaei, A., et al., *On the use of cyclic shear, bending and uniaxial tension–compression tests to reproduce the cyclic response of sheet metals.* Proceedings of the Institution of Mechanical Engineers Part B Journal of Engineering Manufacture, 2014. **229**: p. 453-462.

[9] Yoon, J., et al., *Anisotropic Strain Hardening Behavior In Simple Shear For Cube Textured Aluminum Alloy Sheets.* International Journal of Plasticity - INT J PLASTICITY, 2005. **21**: p. 2426-2447.

[10] Bouvier, S., et al., *Simple shear tests: Experimental techniques and characterization of the plastic anisotropy of rolled sheets at large strains.* Journal of Materials Processing Technology, 2006. **172**: p. 96-103.

[11] Yin, Q., et al., *A cyclic twin bridge shear test for the identification of kinematic hardening parameters.* International Journal of Mechanical Sciences, 2012. **59**: p. 31-43.

[12] Thuillier, S. and P.-Y. Manach, *Comparison of the work-hardening of metallic sheets using tensile and shear strain paths.* International Journal of Plasticity, 2009. **25**(5): p. 733-751.

[13] Aitchison, C.S., Tuckerman, L.B, *The pack method for compressive tests of thin specimens of materials used in thin-wall structures,*. 1939, National Advisory Committee on Aeronautics: Washington, DC,. p. 133-14.

[14] Jackman, K.R., *Improved methods for determining the compression properties of sheet metal,.* Automotive and aviation industries 90, 1944. **11**: p. 36-38

[15] Tozawa, Y., *Plastic Deformation Behavior under Conditions of Combined Stress*, in *Mechanics of Sheet Metal Forming: Material Behavior and Deformation Analysis*, D.P. Koistinen and N.-M. Wang, Editors. 1978, Springer US: Boston, MA. p. 81-110.

[16] Yoshida, F., T. Uemori, and K. Fujiwara, *Elastic–plastic behavior of steel sheets under in-plane cyclic tension–compression at large strain.* International Journal of Plasticity, 2002. **18**(5): p. 633-659.

[17] Boger, R.K., et al., *Continuous, large strain, tension/compression testing of sheet material.* International Journal of Plasticity, 2005. **21**(12): p. 2319-2343.

[18] Boger, R.K., et al., *Continuous, large strain, tension/compression testing of sheet material.* International Journal of Plasticity, 2005. **21**: p. 2319-2343.

[19] Sekine, A. and T. Kuwabara, *Development of In-Plane Reverse Loading Test Apparatus and Measurement of the Bauschinger Effect of Sheet Metals.* The Proceedings of Autumn Conference of Tohoku Branch, 2005. **2005.41**: p. 251-252.

[20] Tritschler, M., et al., *Experimental analysis and modeling of the anisotropic response of titanium alloy Ti-X for quasi-static loading at room temperature.* International Journal of Material Forming, 2014. **7**: p. 259-273.

[21] Hußnätter, W., *Yielding of magnesium alloy AZ31.* Proceedings of ICTP2008, 2009: p. 109.

[22] Cruz, D.J., et al., *Development of a mini-tensile approach for sheet metal testing using Digital Image Correlation.* Procedia Structural Integrity, 2020. **25**: p. 316-323.

[23] Cruz, D.J., *Ensaios mecânicos de tração-compressão em provetes metálicos miniaturizados Desenvolvimento de um equipamento especializado*. 2019.

[24] ISO, *6892-1:2016 Metallic materials — Tensile testing — Part 1: Method of test at room temperature*. 2016.

[25] Yoon, J.W., et al., *Anisotropic strain hardening behavior in simple shear for cube textured aluminum alloy sheets.* International Journal of Plasticity, 2005. **21**: p. 2426-2447.

[26] Kang, J., et al., *Constitutive Behavior of AA5754 Sheet Materials at Large Strains.* Journal of Engineering Materials and Technology, 2008. **130**(3).

[27] Cazacu, O., B. Plunkett, and F. Barlat, *Orthotropic yield criterion for hexagonal closed packed metals.* International Journal of Plasticity, 2006. **22**(7): p. 1171-1194.